

STABILITY ISSUES IN PEAK LIMITING CURRENT MODE CONTROLLED BUCK CONVERTER

Marija Glišić, Predrag Pejović

University of Belgrade, Faculty of Electrical Engineering, Belgrade, Serbia

Abstract: Peak limiting current mode control of a buck converter is reexamined in this paper. It is shown that in the discontinuous conduction mode the conversion ratio determines the converter open loop stability. Furthermore, it is shown that the converter might exhibit limit cycle instability and period multiplication which results in complex behavior and sensitive small signal parameters.

Key Words: Buck Converter / Current Mode Control / Discontinuous Conduction Mode

1. INTRODUCTION

Buck converter loaded by a constant current load, shown in Fig. 1, might expose instability when operated in the discontinuous conduction mode (DCM) applying peak limiting current mode control. The phenomenon occurs in cases when the converter output voltage is $v_{OUT} > v_{IN}/2$, which corresponds to an unstable fixed point. This behavior could be analytically predicted analyzing equations of [1], but practicing engineers are sometimes not familiar with this modeling result. Although the topic is more than 30 years old [2], it attracted attention over decades [3–7]. Detailed analysis is presented in [6], where fairly general case is analyzed, resulting in equations that are sometimes hard to follow. Discrete time model of the converter and bifurcations are analyzed in [7].

Purpose of this paper is to clarify the instability in an easy-to-follow manner, to provide proper models and physical insight in the phenomena, and to identify regions that guarantee period-1 limit cycle operation, regardless the open loop stability.

2. AVERAGING

In the case the buck converter of Fig. 1 is operated applying peak limiting current mode control, waveform of the inductor current in the discontinuous conduction mode is as depicted in Fig. 2. The waveform is obtained assuming that the input voltage and the output voltage are constant over a switching period, and this assumption will hold during the entire analysis presented in this paper. In this manner, the converter is effectively simplified to a switching cell, depicted in Fig. 3, to

compute an average of the inductor current, required to derive dynamic model of the converter. Control variable is maximum of the inductor (i.e., the switch) current I_m , and the average of the inductor current over a switching cycle is related to the converter parameters as

$$\bar{i}_L = \frac{f_S L}{2} I_m^2 \frac{v_{IN}}{v_{OUT} v_{IN} - v_{OUT}} \quad (1)$$

The average value of the inductor current results in a differential equation that governs the output voltage

$$C \frac{d v_{OUT}}{d t} = \frac{f_S L}{2} I_m^2 \frac{v_{IN}}{v_{OUT} v_{IN} - v_{OUT}} - i_{OUT} \quad (2)$$

Setting

$$\frac{d v_{OUT}}{d t} = 0 \quad (3)$$

provides fixed points of the output voltage, and they are

$$v_{OUT1,2} = \frac{v_{IN}}{2} \pm \sqrt{\frac{v_{IN}^2}{4} - \frac{f_S L I_m^2 v_{IN}}{2 i_{OUT}}} \quad (4)$$

Both of the fixed points are within limits

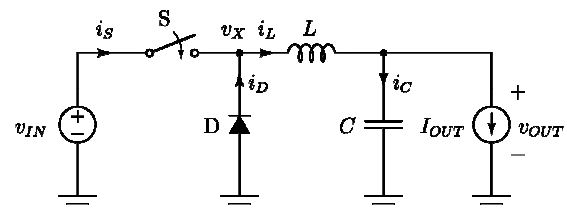


Fig. 1. Buck converter with a constant current load.

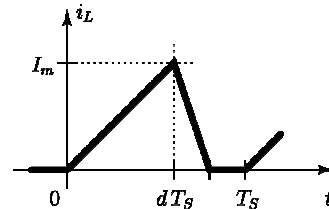


Fig. 2. Inductor current in the DCM.

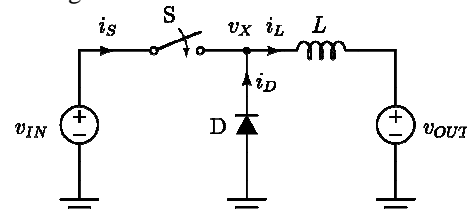


Fig. 3. Buck converter reduced to a switching cell.

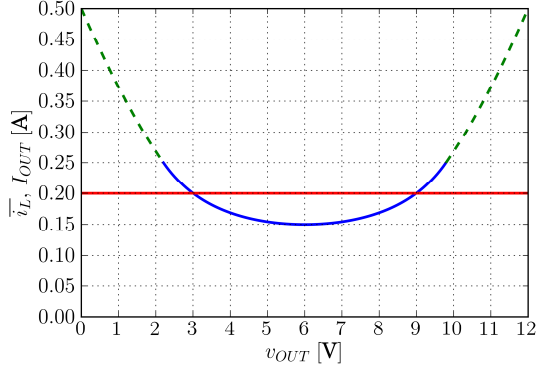


Fig. 4. Dependence $\bar{i}_L(v_{OUT})$ and the fixed points.

$0 < v_{OUT,1,2} < v_{IN}$. One of these fixed points is stable, while the other one is unstable. To gain understanding, let us consider an example of a converter with $v_{IN} = 12\text{ V}$, $L = 36\mu\text{H}$, $f_s = 100\text{ kHz}$, $I_m = 0.5\text{ A}$, $i_{OUT} = 0.2\text{ A}$, $C = 200\mu\text{F}$. In that case, dependence of \bar{i}_L on v_{OUT} is

$$\bar{i}_L = 0.45\text{ A} \frac{12\text{ V}}{v_{OUT}} \frac{1\text{ V}}{12\text{ V} - v_{OUT}} \quad (5)$$

which for $i_{OUT} = \bar{i}_L = 0.2\text{ A}$ provides fixed points of $v_{OUT,1} = 3\text{ V}$ and $v_{OUT,2} = 9\text{ V}$. This example is depicted in Fig. 4, where crossings of $\bar{i}_L(v_{OUT})$ and i_{OUT} indicate fixed points. In the diagram of Fig. 4, the solid blue line corresponds to the converter operating in the discontinuous conduction mode, for $2.2053\text{ V} < v_{OUT} < 9.7947\text{ V}$, while the dashed green line corresponds to the continuous conduction mode. In the discontinuous conduction mode, $\bar{i}_L < I_m/2$, which corresponds to the data of Fig. 4. Hidden assumption in the analysis was that the converter operates in a stable period-1 mode, and \bar{i}_L is computed to correspond to that case. However, this assumption will not be satisfied for the entire operating region $0 < v_{OUT} < v_{IN}$.

3. LINEARIZATION

To analyze stability of the fixed points, linearization [1] of (2) is performed, and after transforming the equation over perturbations in complex domain, it takes form

$$sC\hat{v}_{OUT} = g_{IN}\hat{v}_{IN} + g_{OUT}\hat{v}_{OUT} + \alpha_m\hat{I}_m - \hat{i}_{OUT} \quad (6)$$

where

$$g_{IN} = -\frac{f_s L I_M^2}{2(V_{IN} - V_{OUT})^2} \quad (7)$$

$$g_{OUT} = \frac{f_s L I_M^2 V_{IN} (2V_{OUT} - V_{IN})}{2V_{OUT}^2 (V_{IN} - V_{OUT})^2} \quad (8)$$

and

$$\alpha_m = \frac{f_s L I_M V_{IN}}{(V_{IN} - V_{OUT})V_{OUT}} \quad (9)$$

where V_{IN} , V_{OUT} , and I_M correspond to the values of v_{IN} , v_{OUT} , and I_m at the considered operating point, and

\hat{v}_{IN} , \hat{v}_{OUT} , \hat{I}_m , and \hat{i}_{OUT} represent variations of the corresponding quantities in reference to their value at the operating point.

Rearranging (6), transfer functions of the system

$$\hat{v}_{OUT} = H_{IN}\hat{v}_{IN} + H_m\hat{I}_m - H_{OUT}\hat{i}_{OUT} \quad (10)$$

are obtained as

$$H_{IN} = \frac{g_{IN}}{sC - g_{OUT}} \quad (11)$$

$$H_m = \frac{\alpha_m}{sC - g_{OUT}} \quad (12)$$

and

$$H_{OUT} = -\frac{1}{sC - g_{OUT}}. \quad (13)$$

To provide stability of the transfer functions, it is necessary that $g_{OUT} < 0$, i.e.

$$\frac{d\bar{i}_L}{dv_{OUT}} < 0 \quad (14)$$

which corresponds to downward crossings of $\bar{i}_L(v_{OUT})$ over the load line i_{OUT} . According to (8), this is achieved for

$$V_{OUT} < \frac{1}{2}V_{IN} \quad (15)$$

where $\bar{i}_L(v_{OUT})$ decreases monotonically.

4. DISCRETE TIME MODEL

To analyze the behavior, normalization is applied, such that voltages are normalized to the input voltage as a base quantity,

$$m = \frac{v}{v_{IN}} \quad (16)$$

while currents are normalized to

$$j = \frac{f_s L}{v_{IN}} i. \quad (17)$$

Time variable is normalized to the switching period,

$$\tau = \frac{t}{T_s} = f_s t. \quad (18)$$

In this manner, the inductor equation is from

$$L \frac{dj_L}{d\tau} = v_L \quad (19)$$

normalized to

$$\frac{dj_L}{d\tau} = m_L. \quad (20)$$

Value of m_L is $1 - M$ when the switch is on, $-M$ when the switch is off, and zero when neither the switch nor the diode are on, while $M = v_{OUT}/v_{IN}$ is normalized value of the output voltage. We will also assume that I_m is normalized to J_m , and so forth.

To model the switching cell, let us assume that initial value of the inductor current is $j_0 = j_L(0)$. Our goal is to determine $j_1 = j_L(1)$, assuming that J_m and M are known. To achieve this goal, three cases should be considered.

The first case corresponds to the situation when the switch is on during the whole switching period. Let us compute the time required to get from j_0 to J_m , τ_1 ,

$$\tau_1 = \frac{J_m - j_0}{1 - M}. \quad (21)$$

In the case

$$\tau_1 \geq 1 \quad (22)$$

the switch does not get turned off during the switching period, and corresponding value of j_1 is

$$j_1 = j_0 + 1 - M. \quad (23)$$

Average value of the inductor current during this switching period is

$$\overline{j_L} = \frac{j_0 + j_1}{2}. \quad (24)$$

In the case $\tau_1 < 1$, the switch turns off at τ_1 , and the next relevant time is the time when the inductor current would reach zero. Let us name the time interval j_L requires to get from J_m to 0 as τ_2 ,

$$\tau_2 = \frac{J_m}{M}. \quad (25)$$

In the case

$$\tau_1 + \tau_2 \geq 1 \quad (26)$$

the diode does not turn off till the end of the switching period, and the final value of the inductor current is

$$j_1 = J_m - M(1 - \tau_1) \quad (27)$$

Average value of the inductor current during this switching period is

$$\overline{j_L} = \frac{1}{2}((j_0 + J_m)\tau_1 + (J_m + j_1)(1 - \tau_1)). \quad (28)$$

This is the second of the considered cases. Together with the first case, it consists a group of continuous conduction cases, where $i_L > 0$ during the whole switching period.

On the other hand, if $\tau_1 + \tau_2 < 1$, the case is a discontinuous conduction one, characterized by existence of a time interval where $i_L = 0$. In that case

$$j_1 = 0 \quad (29)$$

and the average of the inductor current during the switching period is

$$\overline{j_L} = \frac{1}{2}J_m(\tau_1 + \tau_2). \quad (30)$$

This concludes analysis of possible cases, where implicit assumption was that $0 < M < 1$. The model consists of the mappings $j_1(j_0, J_m, M)$ and $\overline{j_L}(j_0, J_m, M)$.

All of subsequent numerical results will be obtained using this model, and denormalized to provide diagrams that correspond to the considered converter example.

5. BASINS OF ATTRACTION

To illustrate stability of fixed points, let us follow the introduced example. Depending on the initial condition for the capacitor (i.e., output) voltage, there are two basins of attraction separated by the repelling unstable fixed point. The first basin of attraction applies for the initial conditions $v_{OUT}(0) < 9\text{ V}$, converging towards the

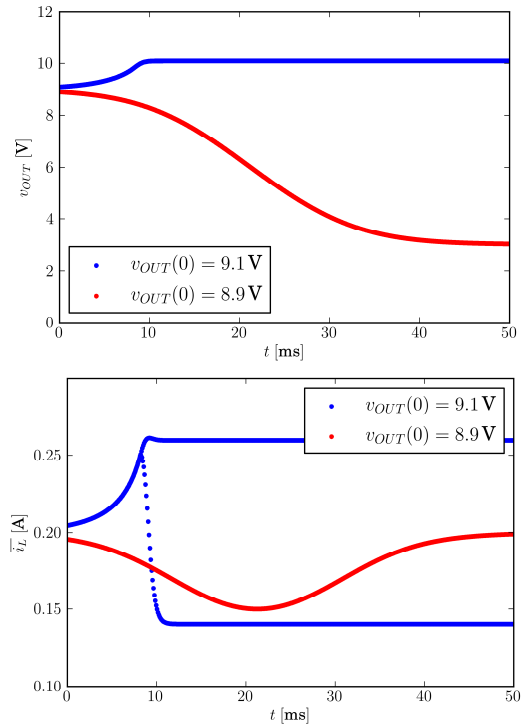


Fig. 5. Waveforms of the output voltage and per-cycle average of the inductor current obtained applying the discrete time converter model.

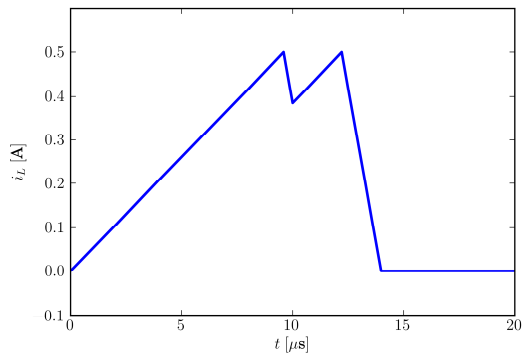


Fig. 6. Steady state waveform of i_L for $v_{OUT}(0) = 9.1\text{ V}$, period doubling.

stable fixed point of $v_{OUT} = 3\text{ V}$. The second basin of attraction applies for $v_{OUT}(0) > 9\text{ V}$, where the output voltage increases, ending up in a period-2 limit cycle for the considered example. To illustrate these effects, simulation of the converter discrete time model is performed for initial values of the output voltage of $v_{OUT}(0) = 8.9\text{ V}$, which corresponds to red curves (dots) in Fig. 5, and $v_{OUT}(0) = 9.1\text{ V}$, which corresponds to blue curves (dots) in Fig. 5.

In Fig. 5, waveform of the output voltage and average of the inductor current over a switching cycle are presented, as a result of a discrete time simulation applying forward Euler integration method with a time step equal to the switching period. It should be underlined here that the average of the inductor current is not a continuous time running average, but discrete time average over a well defined switching period, which starts when the switch is turned on and ends at the subsequent turn on signal for the switch. The transient that corresponds to $v_{OUT}(0) = 8.9\text{ V}$, red line, completes

while the converter operates in the discontinuous conduction mode, in period-1 operation, while in the second transient the converter operation at one point exhibits period-2 bifurcation, resulting in one cycle with one value of \bar{i}_L , followed by a cycle with a different value of \bar{i}_L , while the average of these values in steady state corresponds to the output current. In the second case, for $v_{OUT}(0)=9.1\text{V}$, the output voltage would converge to an analytically obtained limit of $v_{OUT} \approx 10.1232\text{V}$ (to be discussed in further text), while the numerical simulation obtained applying the discrete time model provides $v_{OUT} \approx 10.09\text{V}$, which is a good agreement regarding the simple numerical integration method used. Waveform of i_L over its period of $2T_s$ (period doubling) is shown in Fig. 6, exposing typical “twin peaks” waveform.

6. LIMIT CYCLES

Previous example illustrates that the assumption of period-1 operation introduced to obtain the diagram of Fig. 4 does not hold. Some of the period-1 limit cycles are unstable, and the converter tends to repel them in favor of a stable limit cycle. In the case $0 < i_{OUT} < I_m/2$, which corresponds to the analyzed example, the converter in steady state operates in some sort of discontinuous conduction mode, having an interval of time with the inductor current equal to zero. This allows us to start simulation with the initial condition of the inductor current equal to zero, and to perform simulation until the next zero-current interval is reached. This approach results in the $\bar{i}_L(v_{OUT})$ diagram shown in Fig. 7, which is quite different from the diagram of Fig. 4 in the region that would correspond to the continuous conduction operation for $v_{OUT} > v_{IN}/2$, and exhibits complex behavior. In the diagram of Fig. 7, downward crossing of $\bar{i}_L(v_{OUT})$ line (blue) with the load line (red) at $v_{OUT} \approx 10.1232\text{V}$ corresponds to the stable limit cycle observed in Fig. 5, with i_L shown in Fig. 6.

Analyzing the diagram of Fig. 7, for $J_m < 1/4$ (condition for the DCM to exist) several regions could be identified, as follows:

1. Continuous conduction mode, for

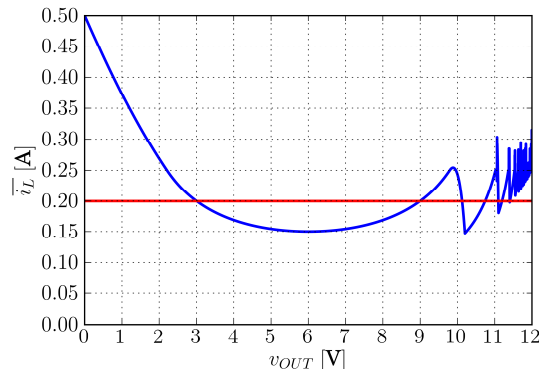


Fig. 7. Dependence $\bar{i}_L(v_{OUT})$ with zero initial conditions.

$$0 < M < \frac{1}{2} - \sqrt{\frac{1}{4} - J_m}. \quad (31)$$

The limit cycle is period-1 and stable, and $\bar{i}_L(v_{OUT})$ is the same as in Fig. 4. The system in open-loop is at the boundary of the stability region (not derived here, [1]).

2. Discontinuous conduction mode, for

$$\frac{1}{2} - \sqrt{\frac{1}{4} - J_m} < M < \frac{1}{2}. \quad (32)$$

The limit cycle is period-1 and stable, and $\bar{i}_L(v_{OUT})$ is the same as in Fig. 4. The system in open-loop is stable.

3. Discontinuous conduction mode, for

$$\frac{1}{2} < M < \frac{1}{2} + \sqrt{\frac{1}{4} - J_m}. \quad (33)$$

The limit cycle is period-1 and stable, and $\bar{i}_L(v_{OUT})$ is the same as in Fig. 4. The system in open-loop is unstable, and compensator should be designed to stabilize the system, [8].

4. Discontinuous conduction mode, for

$$\frac{1}{2} + \sqrt{\frac{1}{4} - J_m} < M < 1 \quad (34)$$

This operation region would correspond to the continuous conduction mode, if the limit cycle had been stable. The limit cycle is period- n , $n > 1$. Dependence $\bar{i}_L(v_{OUT})$ is quite different than shown in Fig. 4.

Although the diagram of Fig. 7 for (34) seems to be fairly complex, significant parts of the curve might be analytically explained in close form. The first case to be analyzed is a family of period- n limit cycles in which the inductor current has triangular waveform. To analyze such cases, let us redefine τ_1 as the time required to reach J_m starting from zero,

$$\tau_1 = \frac{J_m}{1-M} \quad (35)$$

and keep the definition of τ_2 as given by (25). Our goal at this point is to determine regions over M in which the operating mode is discontinuous, and the waveform of i_L is triangular.

The period- n triangular waveform DCM starts at the value of M where $\tau_1 = n-1$, taking $n-1$ switching periods to charge the inductor, which discharges during the n -th switching period, $\tau_2 < 1$. This type of response ends when $\tau_1 + \tau_2 = n$. These two conditions restrict the range of M where period- n triangular waveform of the inductor current is achieved to

$$1 - \frac{J_m}{n-1} < M < \frac{1}{2} + \sqrt{\frac{1}{4} - \frac{J_m}{n}} \quad (36)$$

resulting in the inductor current average

$$\bar{j}_L = \frac{J_m^2}{2nM(1-M)}. \quad (37)$$

In Fig. 8, numerically obtained result is plotted in blue dots, while the analytically obtained results are shown in thin line. Dependence (37) is plotted for n up to 10 in

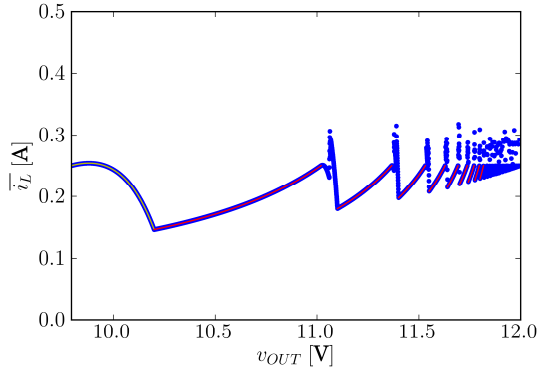


Fig. 8. $\bar{i}_L(v_{OUT})$ comparison of the numerical and the analytical solution.

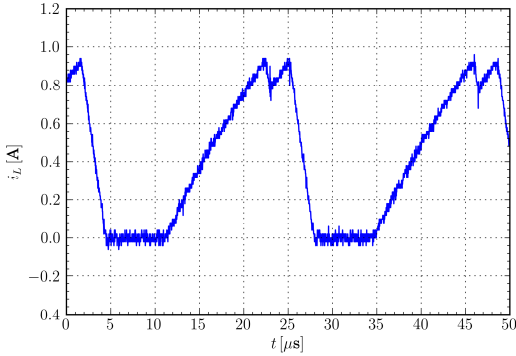


Fig. 9. Waveform of i_L , experimental result, period doubling.

thin red line, and perfectly fits the numerically obtained data where applicable.

In the same manner, the “twin peaks” waveform, shown in Fig. 6, which characterizes period-2 operation that occurs between the period-1 triangular and period-2 triangular waveforms, for

$$\frac{1}{2} + \sqrt{\frac{1}{4} - J_m} < M < 1 - J_m \quad (38)$$

could be analyzed. In that case,

$$\tau_1 = \frac{J_m}{1 - M} \quad (39)$$

$$\tau_2 = 1 - \tau_1 \quad (40)$$

$$j_1 = J_m - M \tau_2 \quad (41)$$

$$\tau_3 = \frac{J_m - j_1}{1 - M} \quad (42)$$

and

$$\tau_4 = \frac{J_m}{M}. \quad (43)$$

Average value of the inductor current is

$$\bar{j}_L = \frac{1}{2} (J_m \tau_1 + (J_m + j_1) \tau_2 + (j_1 + J_m) \tau_3 + J_m \tau_4). \quad (44)$$

Expressing j_1 , τ_1 , τ_2 , τ_3 , and τ_4 in terms of J_m and M , dependence of \bar{j}_L on M is obtained as

$$\bar{j}_L = \frac{2M^2 - 4M + 1}{4(1 - M)^3 M} J_m^2 + \frac{1}{2(1 - M)^2} J_m - \frac{M}{4(1 - M)} \quad (45)$$

which is plotted in Fig. 8 in thin yellow line, and perfectly fits the numerically obtained curve.

To verify the analytical results, an experimental setup is built, and several conclusions are tested, including the period doubling, as shown in Fig. 9.

7. CONCLUSIONS

In this paper, peak limiting current mode control implemented in a buck converter is analyzed, focusing the discontinuous conduction mode. Averaged and linearized averaged converter model are derived assuming constant current load, and it is shown that to provide stable open loop behavior curve $\bar{i}_L(v_{OUT})$ should cross the load line in a downward fashion. It is shown that the open loop transfer functions are stable for $v_{OUT}/v_{IN} < 1/2$, and that the response is unstable with period-1 limit cycle for $1/2 < v_{OUT}/v_{IN} < 1/2 + \sqrt{1/4 - f_s L I_m / v_{IN}}$. Further increases in the output voltage result in complex behavior, with period multiplication and oscillatory dependence of $\bar{i}_L(v_{OUT})$, thus with hard to predict open loop stability and low robustness of the linearized model. Thus, this operating mode should be avoided in practice, in order to keep the switching frequency and the output voltage ripple under control.

5. REFERENCES

- [1] R. W. Erickson, D. Maksimović, *Fundamentals of Power Electronics*, 2nd Ed., Kluwer, Norwell, MA, 2001.
- [2] C. W. Deisch, “Simple switching control method changes power converter into a current source,” *IEEE PESC’78*, 1978, pp. 300–306.
- [3] F. D. Tan, R. D. Middlebrook, “A unified model for current-programmed converters,” *IEEE Transactions on Power Electronics*, vol. 10, pp. 397–408, July 1995.
- [4] J. Sun, D. M. Mitchell, M. F. Greuel, P. T. Krein, R. M. Bass, “Modeling of PWM converters in discontinuous conduction mode—A reexamination,” *IEEE PESC’98*, 1998, pp. 615–622.
- [5] D. Maksimović, S. Čuk, “A unified analysis of PWM converters in discontinuous modes,” *IEEE Transactions on Power Electronics*, vol. 6, pp. 476–490, May 1991.
- [6] T. Sunito, “Analysis and modeling of peak-current-mode-controlled buck converter in DICM,” *IEEE Transactions on Industrial Electronics*, vol. 48, February 2001, pp. 127–135.
- [7] C.-C. Fang, “Unified discrete time modeling of buck converter in discontinuous mode,” *IEEE Transactions on Power Electronics*, vol. 26, pp. 2335–2342, August 2011.
- [8] G. F. Franklin, J. D. Powell, A. Emami-Naeini, *Feedback Control of Dynamic Systems*, 6th Ed., Pearson Higher Education, Upper Saddle River, NJ, 2009.